ELECTRO: A SW TOOL FOR THE ELECTRIC PROPULSION TRAJECTORY OPTIMISATION

Juan C. Bastante, Pelayo Penarroya

OHB System AG, Universitätsallee 27-29, 28359 Bremen, Germany

ABSTRACT

Low-thrust orbit transfers are becoming increasingly attractive thanks to the mass savings they offer and the maturity of electric propulsion technology. For this reason, there is an interest in developing fast, but still reliable trajectory optimisation methods that can be applied in the preliminary phase of the design of a mission. The tool presented is based on the averaging of the equations of motion written in equinoctial elements over true longitude. The calculus of variations is used to identify the optimal control law. In particular, the indirect optimisation method used here is based on a sequential gradient-restoration algorithm. Perturbations such as zonal gravity harmonics are included as well as shadowing effects, which need to be modelled because electric propulsion is normally switched off during eclipses. For the eclipse detection algorithm, an analytical formulation for the extreme points of the eclipse is mandatory, since the entry to and exit from the eclipse set up the limits of integration for the averaging. Further, low-thrust trajectories require a continuous variation of the thrust direction and this has to be compatible with the capabilities of the attitude control system of the satellite. This constraint can be formulated in terms of maximum angular rate for the satellite axes, maximum angular momentum and/or maximum torque. A discussion on how to cope with these constraints in the optimisation method is presented. The capabilities of the developed tool are illustrated with examples of transfers to Geostationary Earth orbit (GEO).

Index Terms— Trajectory Optimisation, Low-Thrust, Electric Propulsion, Indirect Methods

1. INTRODUCTION

In the last years, electric propulsion is becoming an interesting alternative to the traditional chemical propulsion for different applications ranging from interplanetary trajectories to transfers to GEO. In particular, thanks to its high specific impulse, electric propulsion offers a significant mass advantage, which, in the scenario of GEO application, can be translated into increased revenue-generating payload (e.g. SES-12) [1] and/or savings in the cost of the launch (e.g. dual launch of Boeing 702SP satellites) [2].

Electric propulsion has been used for more than 15 years to perform station-keeping manoeuvres in GEO, but only in 2015 the first all-electric satellites were launched. The denomination all-electric indicates that electric propulsion is used not only for station keeping, but also for the transfer from the injection orbit (typically, a GTO, for geosynchronous satellites) to GEO, thus fully exploiting the potential for mass reduction associated with this kind of propulsion system.

On the other hand, electric propulsion is associated to much lower level of thrust than chemical propulsion and this has a direct impact on the transfer duration. Whereas a traditional GTO to GEO transfer with chemical propulsion takes around ten days (and usually less than five manoeuvers), the orbit raising performed with electric propulsion requires a period of several months, during which the thrusters are continuously firing. For this reason, the design and the operation of such a transfer have a higher level of complexity than in the case of traditional chemical propulsion. For example, as discussed later, the optimisation of the trajectory is coupled with the attitude control. In addition, a longer transfer time translates into a longer permanence in Low Earth Orbit (LEO) heights (where collision avoidance operations should be in place) and within the Van Allen Belts.

This paper presents ELECTRO (for *ELECtric propulsion TRajectory Optimisation)*, a SW tools developed in OHB System to deal with the design, analysis and trade-off of such trajectories. The optimisation of the transfer is based on the application of a Sequential Gradient Restoration Algorithm (SGRA), an indirect method described in Section 2. It is common practice, as a conservative approach (at least at design stage), to consider that, due to power constraints, electric propulsion is switched off when the spacecraft is in eclipse condition. The analytical method used to locate the eclipse is described in Section 3. Further, the issue of the coupling between trajectory optimisation and attitude control is briefly discussed in Section 4. Finally, an example of the results that can be obtained with the help of the tool is shown in Section 5, for a typical GTO to GEO transfer.

2. SEQUENTIAL GRADIENT RESTORATION ALGORITHM AND PROBLEM STATEMENT

The optimisation method at the core of ELECTRO is the Sequential Gradient Restoration Algorithm (SGRA), an indirect method developed in the '60 by Miele [3]. Adopting the classical formalism for optimisation problems and assuming that the integration time is normalised, the cost function can be written as:

$$J = \int_0^1 f(x,u,\pi,t)dt + [h(z,\pi)]_0 + [g(x,\pi)]_1 \quad (1)$$

where x denotes the state vector, u is the control vector, π is the vector of parameters, and time has been normalised to run between 0 and 1 (typically transfer time is a parameter provided as a result by the optimisation, i.e., it is contained inside π). This functional J is minimised in presence of differential constraints (dynamics),

$$\dot{x} = \phi(x,u,\pi,t) \quad (2)$$

boundary conditions (initial & final orbits),

$$\begin{aligned} &y(0) = \text{given} \\ &[\zeta(x,\pi)]_0 = 0 \\ &[\psi(x,\pi)]_1 = 0 \end{aligned} \quad (3)$$

and (quality or inequality) path constraints:

$$S(x,u,\pi,t) = 0. \quad (4)$$

The main idea of the method is to alternate Restoration and Gradient phases. In the first phase, the objective is to achieve a feasible transfer, i.e. to fulfil all the constraints (dynamics, boundary & path constraints). In the second phase, the reduction of a cost function, formulated as a function of the state, control and parameters, is sought.

Given that, in general, the system (1)-(4) is non-linear, approximate methods are employed to find a solution iteratively. In particular, the two following errors, referred respectively to the constraints (P) and to the optimality conditions (Q), are defined [3]

$$P = \int_0^1 N(\dot{x} - \phi)dt + \int_0^1 N(S)dt + N(\zeta)_0 + N(\psi)_1 \quad (5)$$

$$\begin{aligned} Q = &\int_0^1 N(\dot{\lambda} - f_x + \phi_x\lambda - S_x\rho)dt + \\ &+ \int_0^1 N(f_u - \phi_u\lambda + S_u\rho)dt + \\ &+N[\int_0^1 N(f_\pi - \phi_\pi\lambda + S_\pi\rho)dt + \\ &+(h_\pi + \zeta_\pi\sigma)_0 + (g_\pi + \psi_\pi\mu)_1] + \\ &+N(-\gamma + h_z + \zeta_x\sigma)_0 + N(\lambda + g_x + \psi_x\mu)_1 \end{aligned} \quad (6)$$

with $N(\nu) = \nu^T\nu$. The algorithm runs until P and Q are smaller than a pre-defined threshold level.

An interesting feature of SGRA is that the initial solution, provided by the user, can be unfeasible (i.e. it can violate any, or even all, of the differential constraints, path constraints and boundary conditions). This means that, differently from other indirect methods, SGRA does not require a good initial solution to converge because the initial restoration phase will correct the provided guess solution to make it feasible. In this way, the dependence on the initial solution is greatly reduced.

Due to the typically high specific impulse of electric propulsion, the transfer problem optimisation is normally formulated as the minimisation of the time required from the injection orbit to GEO. The state vector x contains the mass and the five slow-changing equinoctial elements (a,h,k,p,q) averaged over one orbit. The equinoctial elements h,k,p,q are defined as in [4]

$$\begin{aligned} h &= e\sin(\omega + \Omega) \\ k &= e\cos(\omega + \Omega) \\ p &= \tan\left(\frac{i}{2}\right)\sin(\Omega) \\ q &= \tan\left(\frac{i}{2}\right)\cos(\Omega) \end{aligned} \quad (7)$$

The control vector u contains the corresponding five Lagrange coefficients in the Hamiltonian formulation on the averaged equinoctial elements, whereas the parameter vector is composed by the transfer duration. The boundary conditions at the extreme points are the injection orbit provided by the launcher and the target orbit in GEO.

The perturbation due to the Earth oblateness is modelled considering the contribution of the J2 term and, in particular, its secular effect. In particular, the method of averaging described in [5] was applied; a similar approach will be used in the future to include additional tesseral harmonics and the effect of third-body perturbations.

3. ECLIPSE MODELLING

As already mentioned, the trajectory propagation is carried out assuming that the electric propulsion is switched off while the spacecraft is in eclipse. In this condition, the variation of the orbital elements due to thrust is not obtained by performing the average over the whole orbit

$$\bar{\dot{a}} = \frac{1}{2\pi}\int_0^{2\pi} f_a dF \tag{8}$$

but only on the part outside the eclipse region

$$\bar{\dot{a}} = \frac{1}{2\pi}\int_{F_1}^{F_0} f_a dF \tag{9}$$

as represented in Fig. 1. In the current work, it is assumed that F_0 and F_1 are the extreme points of the eclipse obtained with a cylindrical model for the shadow, where F stands for eccentric longitude (i.e., addition of right ascension of ascending node, argument of perigee and eccentric anomaly).

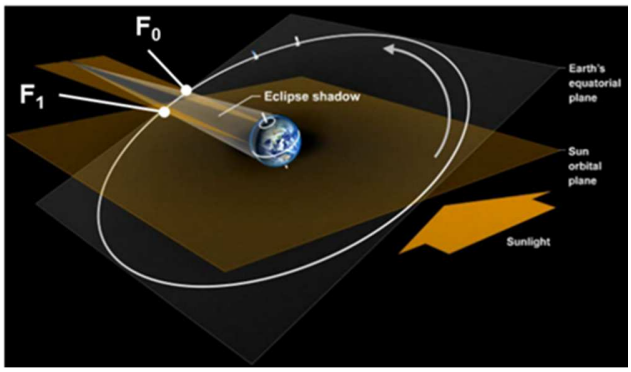

Figure-1: Representation of the eclipse condition and of the eclipse extreme points. Figure readapted from the COMET project, http://meted.ucar.edu/ of the University Corporation for Atmospheric Research (UCAR)

With respect to the formulation with no eclipses, the dynamics is obviously changed. By looking at the equations (5) and (6), one can observe how the optimisation method requires not only the expression of the new dynamics, but also the derivative of the dynamics with respect to state, control and parameters. For this reason, an analytical approximation of the F_0 and F_1 points, as a function of the state vector, together with the corresponding partial derivatives of the eclipse location with respect to the state vector, has to be derived.

The problem is represented on the orbital plane, as shown in Fig. 2. The x-axis of the orbital plane points towards the Sun direction, so the half-ellipse representing the shadow is aligned to the x-axis; the ellipse representing the orbit can have any orientation on the plane.

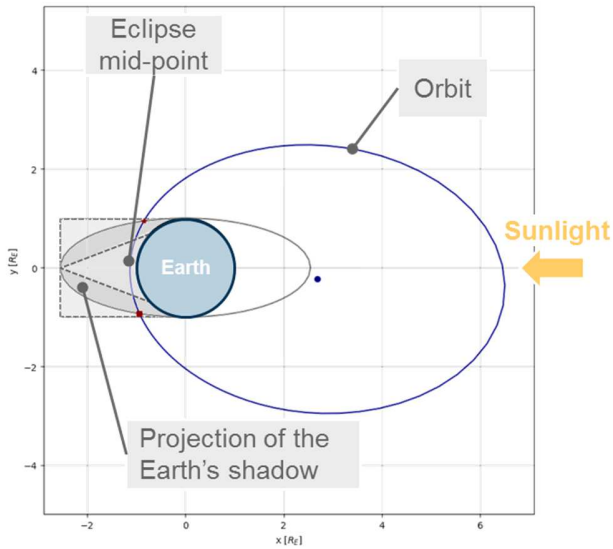

Figure-2: Representation of the elliptical shadow on the orbital plane.

Finding F_0 and F_1 requires determining the intersection points between the two ellipses in Fig. 2 (i.e. orbit and shadow). This can easily be done numerically, whereas a closed analytical form is only available for generic values of the coefficients of the two ellipses if solving for the corresponding quartic equation. Former versions of ELECTRO contained an implementation of the eclipse points based on the combination of two solutions: intersection of the orbit with a rectangular shadow, and with triangular shadow (as illustrated in Fig. 2). By a proper interpolation of these two solutions, a fast a moderately accurate solution could be obtained.

Current implementation, however, solves for the quartic itself [6], detecting the number of real intersections between the two involved ellipses (from 0 to 4), filtering out those solutions which do not result in an eclipse, and deriving the corresponding derivatives of F0 and F1 with respect to the state variables (averages equinoctial elements) in a smooth and continuous way.

4. AOCS CONSTRAINTS

The transfer profiles generated by ELECTRO are given in the form of a thrust vector and magnitude to be implemented along time (control variables) to obtain a certain optimal evolution of the equinoctial elements (state vector) in a given optimised transfer time (parameter vector). As a consequence, this profile can be regarded as the evolution along time of a force in the three-dimensional space, which can be resembled with one satellite axis, pointing in the direction of the electric propulsion thrusters.

It follows from this reasoning that the optimisation of the thrusting law is implicitly fixing one of the satellite axes along time. The only remaining degree of freedom to fully determine the attitude profile of the satellite is just the rotation around this thrust direction which, in principle, is not necessarily related to the optimal change of the orbital elements, but with other variables of the satellite operation (for instance, power balance and Sun Aspect Angle, SAA). The typical solution, also because of the high power demand from electric propulsion, is to rotate the satellite around the thrust in order to have also perfect pointing of the solar panels to the Sun, providing the longitudinal axes of the solar generators is orthogonal to the thrust direction. By doing so, and particularly at some points & situations resulting in a fast dynamics of the satellite (for instance, during perigee passage, or when Sun is seen with a low elevation from the orbital plane), it might happen that the attitude profile (3D, i.e., thrust direction plus rotation around thrust) is not flyable because of AOCS limitations. These can be typically expressed in terms of maximum values (at attitude guidance level) of the angular momentum

$$L = I\tilde{\omega} \tag{10}$$

and torque

$$T = I\frac{d\tilde{\omega}}{dt} + \tilde{\omega} \times L. \tag{11}$$

Besides of these constraints, power requirements prescribe a good SAA profile, allowing the maintenance of a high level of charge for the batteries under all situations. As a consequence, the trade-off between the (potentially fast) dynamics required by the thrusting profile and the SAA, on one side; and the limits imposed by AOCS subsystem, on the other, needs to be addressed in detail.

To this end, several aspects must be considered. First, the option of carrying out a six-degree of freedom propagation and/or optimisation might represent a burden because the computational time would be too large and not in line with the objective of developing fast tools for mission analysis tasks.

Second, it has to be found a coherency between the averaging approach and the fact that these AOCS constraints are to be imposed in specific points inside one orbit. Precisely because of this, and considering the averaging approach adopted by the ELECTRO tool, it would probably make not much sense to condition the thrusting profile during the full revolution just to avoid a constraint violation in a given specific point or short interval lasting few minutes. As a consequence, and even though the SGRA algorithm would allow the implementation of this constraint at optimisation level, the need of having such constraint would probably mean a non-adequate sizing of the attitude guidance actuators, since it would necessarily imply to run the transfer with sub-optimal solutions.

On the other hand, if implementing the rotation around the thrust as fast as needed by the perfect pointing to the Sun, the AOCS constraints will most likely be violated at some specific intervals during transfer. For instance, during perigee passage (imposing a faster dynamics also for thrust, and hence letting a tighter margin for the rotation around thrust), or when the thrust vector points at or close to the Sun. As a consequence, a smoothing strategy [7] is needed to generate the complete attitude profile compatible with those constraints, taking as input the thrusting profile generated by the optimiser.

Fig. 3, Fig.4 and Fig. 5 illustrate the smoothing of the attitude profile performed by ELECTRO to comply with AOCS constraints. The cost of this smoothing, in terms of delta-v, is null, since the thrust profile is not modified. The only impact appears on the power balance (i.e., a slightly lower charge state in the batteries during some short intervals), but due to the short duration of these intervals in normal conditions (up to one hour, in a GTO to GEO worst case), batteries should easily recover the optimum state shortly after recovering the optimal pointing to the Sun.

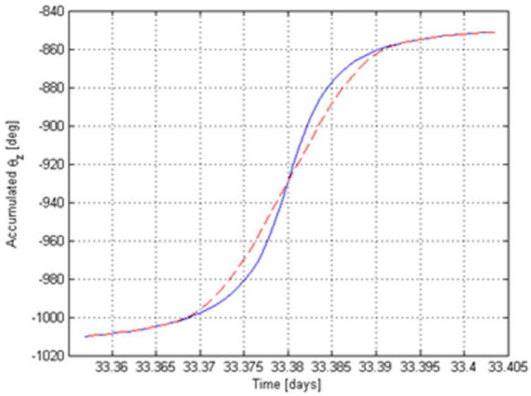

Figure-3: Accumulated rotation around thrust vector. Original profile in blue, smoothed in dashed red

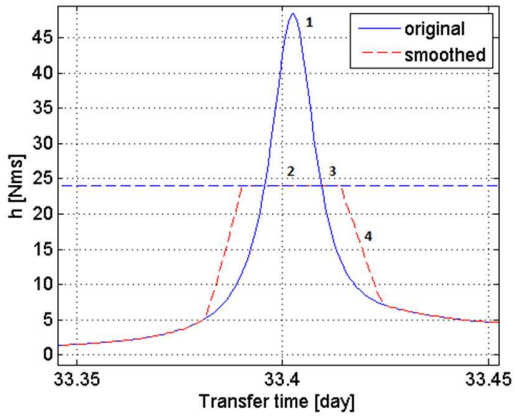

Figure-4: Angular momentum evolution. Original profile in blue, smoothed in dashed red

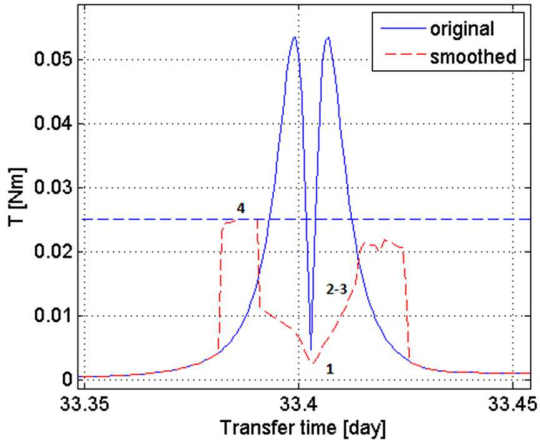

Figure-5: Torque evolution. Original profile in blue, smoothed in dashed red

5. OUTPUTS GIVEN BY ELECTRO

Once eclipses and perturbations are included in the dynamics as described above, the optimiser can be run to generate different transfer trajectories for the scenarios under analysis. The optimiser provides as output the guidance law for the spacecraft in terms of two angles (i.e. α and β) that define the orientation of the thrust vector in space. When the thrusters are on, the maximum thrust is delivered. The thrusters are always on except for eclipses. For this reason, the minimisation of the Δv described in Section 2 becomes equivalent to the minimisation of the required transfer time, which is common practice for electric propulsion (because of the high Isp). The optimisation of a transfer trajectory with the current settings, and starting from an initial solution violating all the dynamics constraints and the final boundary condition takes few minutes (around 10) on a desktop with four CPUs at 3.40GHz.

Given the evolution of the thrust vector, the full satellite attitude is derived by orienting the spacecraft in such a way that the solar panels are perpendicular to the Sun-satellite direction (or as close as possible), unless in the cases in which the AOCS constraints force it to be different, as explained in Section 4. The ability of performing this rotation depends on the attitude control authority, which is driven by the satellite inertias and constrained by the attitude actuators in charge of the feed forward profile. By following this process, the orbit evolution and the attitude history of the satellite is known and the transfer can be fully characterised. In particular, typical outputs of the tool include:

- Thrust profile
- Evolution of equinoctial elements
- Evolution of position & velocity
- Eclipse profile in terms of location and duration along the transfer
- Angular velocity in body axes
- SADM actuation profile (angle & angular rate)
- Star trackers' blinding profile
- 3D visualisation of the trajectory
- Preliminary estimation of the collision probability with space debris [8]
- Launch window analysis
- Number of GEO ring crossings

The core algorithms of the tool are coded in C, whereas Python and MATLAB are used for data visualisation and post-processing. To illustrate the type of results in ELECTRO, a classical GTO to GEO transfer is considered.

Fig. 6 shows a 3D visualisation of the transfer, where the colour indicates the time elapsed from the launch. The black region indicates the eclipses. For this case, the perigee of the orbit is positioned behind the Earth wrt the Sun at the beginning, which guarantees short eclipses. Fig. 7 presents the corresponding eclipse duration along the transfer.

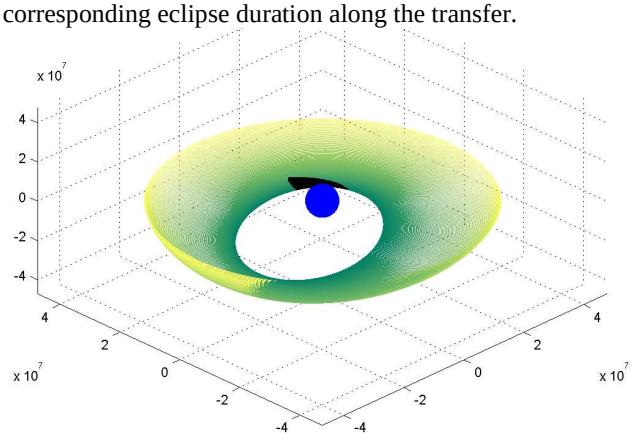

Figure-6: 3D visualisation of a GTO to GEO transfer. Colour denotes elapsed time since launch, black indicates eclipse

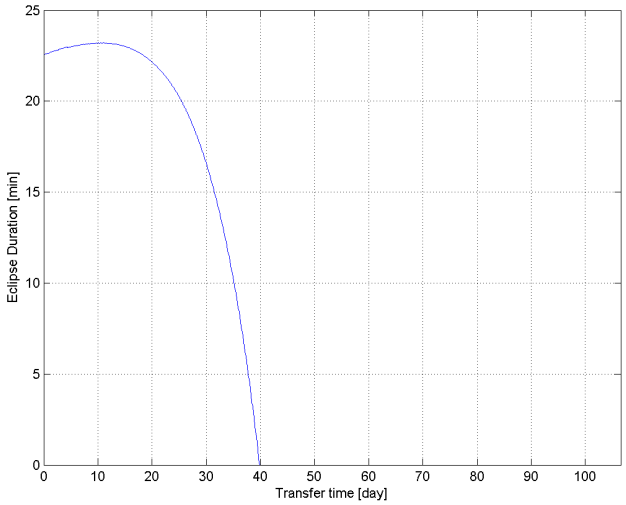

Figure-7: Eclipse duration profile

As already mentioned, the tool provides the evolution of the thrust vector: Fig. 8 shows the evolution of its component in Radial (R), Along Track (T) & Across Track (C) reference system, during the first day of the transfer and Fig. 9 the evolution during the last day. One can observe how the variation of the thrust direction is much quicker in the first phase of the transfer, especially in correspondence to the perigee passages. Another confirmation of this behaviour is presented by the evolution of the angular velocity presented in Fig. 10: during the first 40 days of the transfer, the angular momentum is significantly higher. As a consequence, the spacecraft losses the perfect pointing to the Sun during some few minutes for the orbits in which the maximum allowed value of angular momentum is reached.

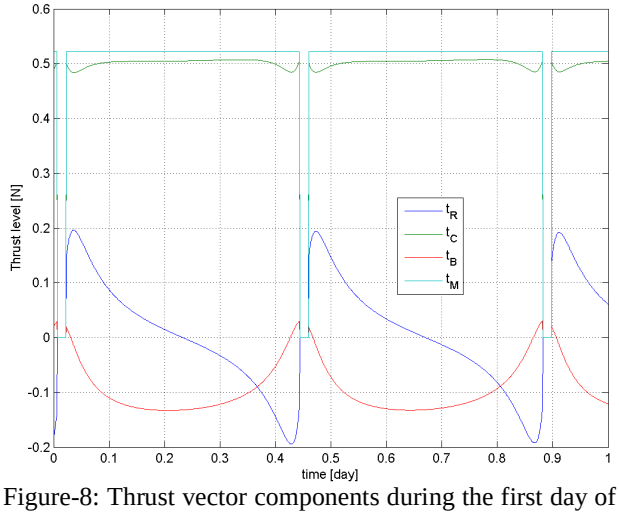

Figure-8: Thrust vector components during the first day of a GTO to GEO transfer

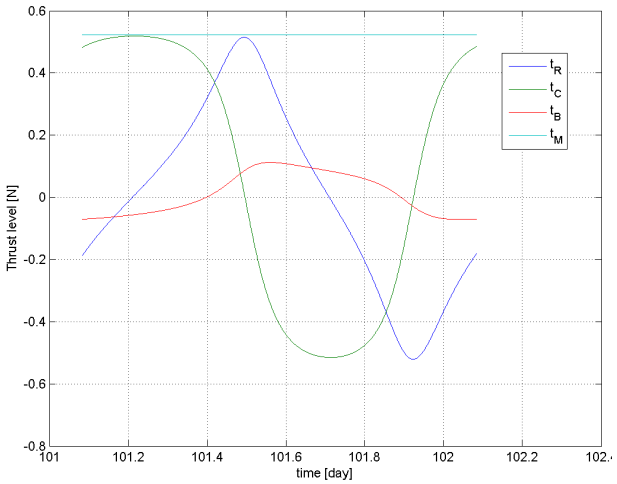

Figure-9: Thrust vector components during the last day of a GTO to GEO transfer

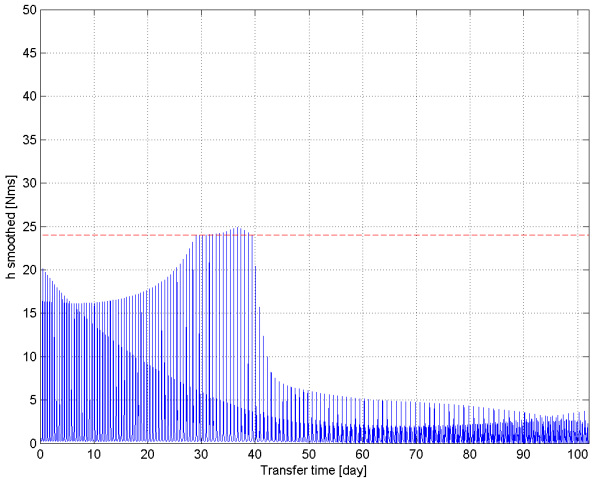

Figure-10: Angular momentum profile for a GTO to GEO transfer

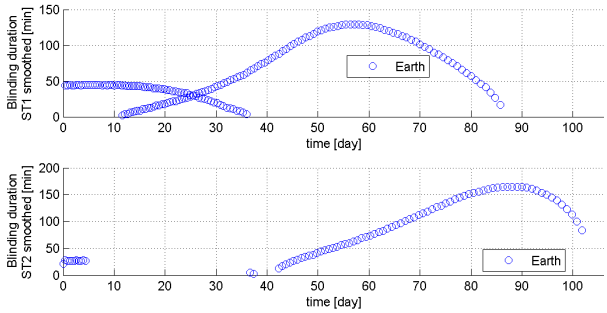

Figure-11: Blinding profiles for the two star trackers on board the satellite during a GTO to GEO transfer. Only Earth blinding are detected.

Also, by providing the tool with the orientation in body axes of sensors, e.g. star trackers, the corresponding blinding profiles can be computed. For example, Fig. 11 shows when the star trackers are blinded by either the Earth or the Sun; only Earth blinding events are detected in this example. The same analysis also provides the duration of all the detected blinding conditions.

Crossing with the GEO ring is in principle to be avoided, since it would somehow constrain the operation of the satellite during the transfer and interfere with other in service satellites. The number and duration of this GEO crossing is also provided as part of the outputs of ELECTRO, as illustrated by Fig. 12 and Fig. 13.

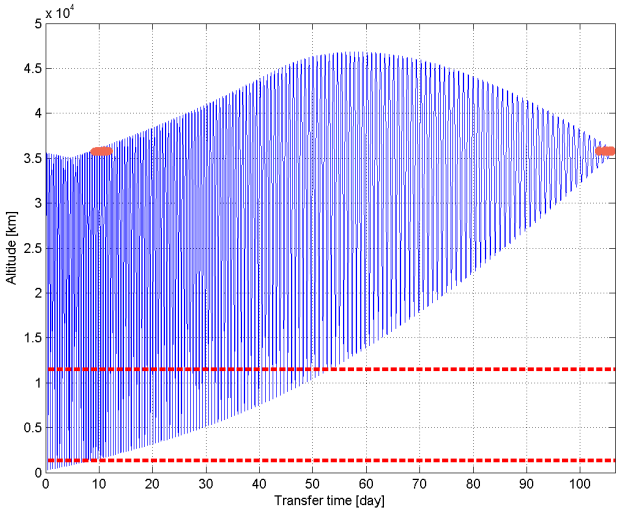

Figure-12: Altitude evolution during a GTO to GEO transfer; orange markers refer to GEO ring crossing, while dashed red lines delimit the Van Allen belt heights

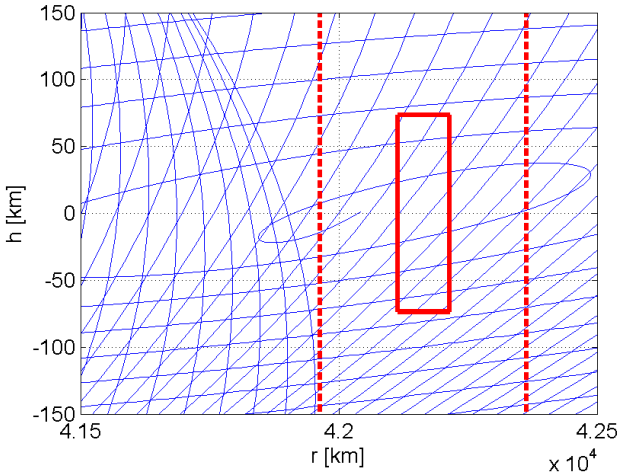

Figure-13: GEO ring crossings during a GTO to GEO transfer

Blinding conditions and eclipses are affected by the launch epoch, so the tool can also perform a launch window analysis to obtain results that are more general than studying a transfer scenario at a single epoch. For example, the launch window can be restricted to avoid transfers with a too long star tracker blinding time or a too long time in eclipse.

Fig. 14 shows the launch window analysis performed to study the variation of the accumulated time spent in eclipse (expressed as a percentage of the total transfer duration) as a function of the hour and day of launch. To generate this kind of results, the optimiser can be run in continuation (for a new eclipse profile) from one cell to the other, meaning that the optimised solution at the previous cell can be used as initial condition for the new optimisation. To produce the results in Fig. 12, more than 1770 trajectories would be needed. An alternative approach is to optimise only one trajectory and rotate for the different launch opportunities to compute the corresponding eclipse profile – this approximation provides good enough eclipse statistics. Fig. 15 shows the same launch window analysis, this time for the longest eclipse during transfer. These distributions can then be used to support the subsystems in the verification of their configuration (e.g. for battery sizing).

	0	1	2	3	4	5	6	7	8	9	10	11	12	13	14	15	16	17	18	19	20	21	22	23
0	2.33	2.30	2.30	2.33	2.40	2.51	2.65	2.81	2.91	2.56	2.33	2.20	2.10	2.02	1.93	1.84	1.77	1.72	1.75	2.03	2.49	2.51	2.45	2.38
5	2.27	2.24	2.24	2.27	2.35	2.46	2.61	2.79	2.94	2.70	2.46	2.32	2.21	2.11	2.01	1.91	1.85	1.80	1.87	2.40	2.55	2.50	2.41	2.32
10	2.21	2.18	2.18	2.22	2.29	2.40	2.56	2.75	2.94	2.85	2.59	2.44	2.31	2.20	2.09	1.99	1.92	1.89	2.06	2.56	2.56	2.46	2.36	2.27
15	2.15	2.12	2.12	2.16	2.23	2.35	2.51	2.71	2.93	3.00	2.72	2.56	2.42	2.29	2.17	2.08	2.01	2.01	2.45	2.62	2.53	2.41	2.29	2.20
20	2.09	2.06	2.06	2.10	2.17	2.29	2.45	2.66	2.91	3.09	2.86	2.68	2.53	2.38	2.26	2.16	2.11	2.15	2.64	2.62	2.49	2.35	2.23	2.13
25	2.02	2.00	2.00	2.04	2.11	2.23	2.39	2.60	2.86	3.11	2.99	2.80	2.63	2.47	2.34	2.26	2.23	2.41	2.69	2.58	2.42	2.27	2.16	2.07
30	1.96	1.93	1.94	1.98	2.05	2.17	2.33	2.54	2.80	3.09	3.13	2.91	2.73	2.56	2.44	2.36	2.37	2.70	2.67	2.51	2.34	2.20	2.08	1.99
35	1.89	1.87	1.88	1.92	1.99	2.10	2.26	2.47	2.73	3.04	3.24	3.03	2.83	2.66	2.53	2.47	2.55	2.75	2.61	2.43	2.26	2.11	2.00	1.93
40	1.82	1.81	1.82	1.86	1.93	2.04	2.19	2.39	2.64	2.95	3.23	3.13	2.92	2.74	2.62	2.60	2.78	2.71	2.52	2.33	2.17	2.03	1.93	1.85
45	1.76	1.75	1.76	1.80	1.87	1.97	2.11	2.30	2.54	2.83	3.13	3.22	3.00	2.83	2.72	2.74	2.80	2.62	2.42	2.23	2.07	1.94	1.85	1.78
50	1.70	1.69	1.70	1.74	1.81	1.90	2.03	2.20	2.41	2.67	2.96	3.18	3.07	2.91	2.83	2.86	2.71	2.50	2.30	2.12	1.97	1.86	1.77	1.72
55	1.63	1.63	1.64	1.68	1.74	1.83	1.95	2.09	2.27	2.49	2.74	2.98	3.08	2.99	2.91	2.77	2.57	2.36	2.17	2.01	1.88	1.77	1.70	1.65
60	1.57	1.57	1.59	1.62	1.68	1.76	1.85	1.97	2.11	2.27	2.46	2.69	2.86	2.88	2.77	2.60	2.40	2.20	2.04	1.89	1.78	1.69	1.63	1.58
65	1.51	1.51	1.53	1.56	1.61	1.68	1.76	1.84	1.93	2.01	2.14	2.33	2.55	2.60	2.54	2.39	2.21	2.05	1.91	1.79	1.69	1.61	1.56	1.52
70	1.46	1.46	1.48	1.51	1.55	1.60	1.65	1.70	1.72	1.73	1.78	1.93	2.14	2.26	2.25	2.15	2.02	1.89	1.78	1.68	1.60	1.54	1.49	1.46
75	1.40	1.41	1.42	1.45	1.48	1.52	1.54	1.54	1.50	1.42	1.39	1.50	1.72	1.90	1.96	1.92	1.83	1.74	1.66	1.58	1.52	1.47	1.43	1.40
80	1.36	1.36	1.38	1.40	1.42	1.44	1.43	1.38	1.26	1.10	1.01	1.07	1.30	1.53	1.67	1.69	1.66	1.61	1.55	1.49	1.44	1.40	1.38	1.36
85	1.34	1.39	1.41	1.42	1.44	1.44	1.41	1.30	1.11	0.88	0.72	0.75	0.98	1.27	1.46	1.55	1.57	1.55	1.52	1.48	1.44	1.42	1.40	1.39
90	1.45	1.47	1.49	1.50	1.52	1.50	1.42	1.26	0.99	0.71	0.53	0.53	0.74	1.06	1.32	1.46	1.52	1.53	1.52	1.50	1.48	1.46	1.45	1.46
95	1.55	1.57	1.60	1.62	1.62	1.58	1.46	1.24	0.91	0.61	0.44	0.43	0.59	0.91	1.21	1.40	1.50	1.54	1.55	1.55	1.54	1.54	1.54	1.56
100	1.68	1.71	1.74	1.76	1.75	1.68	1.51	1.23	0.86	0.60	0.57	0.55	0.54	0.81	1.14	1.37	1.50	1.57	1.61	1.62	1.63	1.64	1.66	1.68
105	1.83	1.87	1.90	1.92	1.89	1.79	1.57	1.22	0.86	0.75	0.73	0.70	0.68	0.77	1.10	1.36	1.52	1.62	1.67	1.70	1.73	1.75	1.78	1.82
110	1.99	2.04	2.08	2.10	2.05	1.90	1.62	1.23	0.94	0.91	0.87	0.85	0.82	0.80	1.08	1.36	1.55	1.67	1.75	1.80	1.84	1.88	1.92	1.97
115	2.16	2.23	2.28	2.30	2.23	2.01	1.66	1.24	1.08	1.04	1.00	0.97	0.95	0.92	1.07	1.36	1.58	1.73	1.82	1.89	1.95	2.01	2.06	2.13
120	2.34	2.43	2.52	2.60	2.48	2.12	1.68	1.27	1.20	1.15	1.11	1.07	1.05	1.02	1.08	1.36	1.60	1.77	1.88	1.98	2.05	2.12	2.20	2.28
125	2.50	2.70	2.80	2.76	2.64	2.24	1.67	1.32	1.26	1.20	1.16	1.12	1.10	1.08	1.07	1.32	1.57	1.76	1.90	2.01	2.10	2.19	2.29	2.40
130	2.75	2.88	2.86	2.79	2.65	2.34	1.63	1.35	1.27	1.22	1.17	1.13	1.11	1.09	1.08	1.26	1.52	1.73	1.88	2.01	2.13	2.24	2.37	2.52
135	2.93	2.92	2.86	2.77	2.64	2.36	1.60	1.37	1.29	1.23	1.18	1.15	1.12	1.11	1.10	1.21	1.48	1.70	1.88	2.03	2.17	2.31	2.48	2.80
140	2.97	2.91	2.82	2.73	2.61	2.35	1.60	1.40	1.31	1.25	1.20	1.16	1.14	1.13	1.12	1.18	1.45	1.69	1.89	2.06	2.23	2.42	2.69	3.00
145	2.97	2.87	2.77	2.68	2.57	2.34	1.61	1.43	1.33	1.26	1.22	1.18	1.16	1.15	1.15	1.18	1.43	1.69	1.92	2.12	2.33	2.59	3.02	3.05
150	2.92	2.81	2.71	2.62	2.52	2.33	1.65	1.46	1.35	1.28	1.23	1.20	1.19	1.18	1.18	1.19	1.43	1.71	1.96	2.20	2.47	2.97	3.12	3.04
155	2.86	2.74	2.64	2.56	2.48	2.31	1.70	1.50	1.38	1.31	1.26	1.23	1.21	1.21	1.21	1.24	1.44	1.74	2.03	2.32	2.70	3.18	3.14	2.99
160	2.78	2.66	2.57	2.50	2.43	2.30	1.76	1.54	1.41	1.34	1.29	1.26	1.24	1.24	1.26	1.28	1.47	1.80	2.13	2.49	3.17	3.25	3.10	2.92
165	2.69	2.57	2.49	2.43	2.38	2.28	1.82	1.58	1.45	1.37	1.32	1.29	1.28	1.29	1.30	1.34	1.52	1.88	2.27	2.79	3.34	3.24	3.03	2.83
170	2.60	2.48	2.41	2.37	2.34	2.27	1.90	1.62	1.49	1.41	1.36	1.33	1.32	1.33	1.36	1.40	1.58	1.99	2.47	3.33	3.39	3.18	2.94	2.74
175	2.50	2.40	2.33	2.31	2.29	2.25	2.02	1.68	1.54	1.45	1.40	1.38	1.37	1.38	1.42	1.47	1.67	2.15	2.83	3.53	3.36	3.09	2.84	2.64
180	2.41	2.31	2.26	2.24	2.24	2.23	2.09	1.73	1.59	1.50	1.45	1.43	1.43	1.45	1.49	1.56	1.79	2.38	3.46	3.55	3.28	2.98	2.73	2.53
185	2.31	2.23	2.19	2.18	2.19	2.20	2.13	1.80	1.65	1.56	1.51	1.49	1.50	1.53	1.58	1.67	1.98	2.78	3.67	3.51	3.18	2.86	2.61	2.42
190	2.22	2.14	2.11	2.11	2.14	2.18	2.16	1.87	1.71	1.62	1.57	1.56	1.58	1.62	1.69	1.81	2.23	3.53	3.72	3.41	3.05	2.73	2.49	2.31
195	2.12	2.06	2.04	2.05	2.09	2.15	2.17	1.96	1.78	1.69	1.65	1.64	1.67	1.73	1.82	1.98	2.62	3.88	3.68	3.28	2.90	2.60	2.37	2.21
200	2.03	1.98	1.97	1.99	2.04	2.11	2.17	2.05	1.86	1.77	1.73	1.74	1.78	1.86	1.98	2.19	3.48	3.91	3.56	3.13	2.75	2.46	2.25	2.10
205	1.94	1.90	1.90	1.93	1.99	2.08	2.17	2.16	1.95	1.86	1.83	1.85	1.90	2.01	2.18	2.48	3.95	3.86	3.40	2.95	2.59	2.32	2.13	2.00
210	1.85	1.83	1.83	1.87	1.94	2.04	2.15	2.22	2.05	1.96	1.94	1.97	2.05	2.19	2.42	3.11	4.06	3.72	3.21	2.77	2.43	2.19	2.02	1.91
215	1.77	1.75	1.76	1.81	1.89	2.00	2.13	2.25	2.17	2.08	2.06	2.11	2.22	2.41	2.73	4.01	4.03	3.52	3.00	2.58	2.28	2.06	1.91	1.81
220	1.69	1.68	1.70	1.75	1.84	1.96	2.11	2.26	2.30	2.21	2.21	2.28	2.43	2.67	3.17	4.21	3.86	3.28	2.78	2.40	2.13	1.93	1.80	1.72
225	1.61	1.61	1.64	1.70	1.79	1.92	2.08	2.26	2.41	2.36	2.37	2.48	2.67	3.01	4.03	4.16	3.62	3.02	2.55	2.22	1.98	1.81	1.70	1.63
230	1.54	1.54	1.58	1.64	1.74	1.87	2.05	2.25	2.47	2.53	2.57	2.71	2.97	3.47	4.29	3.95	3.31	2.75	2.33	2.04	1.83	1.69	1.60	1.55
235	1.47	1.48	1.52	1.59	1.69	1.83	2.01	2.23	2.49	2.72	2.79	2.99	3.35	4.13	4.20	3.63	2.98	2.47	2.11	1.87	1.70	1.58	1.51	1.47
240	1.40	1.42	1.46	1.53	1.64	1.78	1.97	2.20	2.49	2.81	3.06	3.33	3.85	4.24	3.90	3.24	2.64	2.20	1.91	1.71	1.57	1.48	1.42	1.39
245	1.33	1.36	1.41	1.48	1.59	1.74	1.93	2.17	2.47	2.84	3.24	3.67	4.05	4.02	3.48	2.81	2.29	1.94	1.71	1.55	1.45	1.37	1.33	1.31
250	1.27	1.30	1.36	1.43	1.54	1.69	1.88	2.12	2.43	2.82	3.26	3.68	3.89	3.60	2.97	2.38	1.96	1.70	1.53	1.41	1.33	1.28	1.25	1.24
255	1.21	1.24	1.30	1.38	1.49	1.64	1.83	2.07	2.38	2.76	3.17	3.51	3.51	3.05	2.43	1.96	1.66	1.48	1.36	1.28	1.22	1.19	1.17	1.17
260	1.16	1.20	1.26	1.34	1.45	1.60	1.79	2.02	2.32	2.67	3.02	3.21	3.00	2.45	1.92	1.58	1.40	1.29	1.22	1.17	1.14	1.12	1.12	1.13
265	1.18	1.23	1.29	1.38	1.49	1.64	1.82	2.05	2.32	2.63	2.88	2.88	2.47	1.90	1.51	1.32	1.24	1.19	1.17	1.15	1.14	1.13	1.14	1.16
270	1.24	1.29	1.36	1.45	1.57	1.71	1.89	2.10	2.34	2.58	2.69	2.47	1.91	1.42	1.20	1.14	1.15	1.16	1.17	1.17	1.17	1.18	1.19	1.22
275	1.33	1.39	1.46	1.55	1.67	1.81	1.98	2.17	2.37	2.52	2.46	2.02	1.38	1.03	0.97	1.03	1.10	1.16	1.20	1.22	1.24	1.26	1.28	1.31
280	1.44	1.50	1.57	1.66	1.78	1.91	2.07	2.24	2.39	2.43	2.18	1.53	0.94	0.77	0.84	0.97	1.10	1.19	1.25	1.30	1.33	1.36	1.38	1.42
285	1.56	1.62	1.69	1.78	1.90	2.03	2.17	2.31	2.40	2.32	1.85	1.09	0.76	0.74	0.80	0.96	1.12	1.24	1.33	1.39	1.43	1.46	1.50	1.54
290	1.68	1.74	1.81	1.91	2.01	2.13	2.26	2.37	2.39	2.17	1.51	0.89	0.90	0.90	0.90	0.99	1.16	1.30	1.41	1.48	1.53	1.57	1.61	1.66
295	1.79	1.85	1.93	2.02	2.12	2.24	2.35	2.42	2.36	1.98	1.20	1.04	1.04	1.04	1.05	1.06	1.22	1.37	1.49	1.57	1.63	1.67	1.72	1.76
300	1.88	1.95	2.02	2.12	2.22	2.33	2.42	2.45	2.31	1.77	1.15	1.16	1.16	1.16	1.17	1.17	1.26	1.42	1.54	1.63	1.70	1.75	1.80	1.84
305	1.91	1.98	2.06	2.16	2.27	2.38	2.46	2.45	2.21	1.53	1.22	1.22	1.22	1.23	1.23	1.23	1.26	1.40	1.53	1.62	1.70	1.75	1.80	1.85
310	1.91	2.00	2.09	2.21	2.34	2.46	2.53	2.47	2.11	1.33	1.27	1.27	1.26	1.27	1.26	1.26	1.38	1.50	1.60	1.67	1.73	1.79	1.85	
315	1.93	2.03	2.15	2.30	2.51	2.65	2.72	2.60	2.04	1.35	1.33	1.32	1.31	1.31	1.31	1.30	1.29	1.36	1.48	1.57	1.65	1.72	1.78	1.85
320	1.97	2.09	2.28	2.49	2.61	2.72	2.79	2.73	2.02	1.43	1.40	1.38	1.37	1.36	1.35	1.34	1.33	1.35	1.46	1.56	1.64	1.71	1.79	1.87
325	2.03	2.24	2.45	2.56	2.65	2.74	2.81	2.78	2.09	1.52	1.47	1.44	1.42	1.41	1.40	1.38	1.36	1.35	1.45	1.55	1.64	1.72	1.81	1.91
330	2.18	2.42	2.51	2.58	2.65	2.74	2.82	2.81	2.29	1.63	1.55	1.51	1.49	1.47	1.45	1.43	1.40	1.38	1.45	1.55	1.64	1.74	1.85	1.99
335	2.38	2.47	2.52	2.57	2.64	2.73	2.81	2.83	2.41	1.75	1.65	1.59	1.55	1.53	1.50	1.47	1.45	1.41	1.45	1.56	1.66	1.78	1.92	2.14
340	2.44	2.48	2.51	2.55	2.62	2.71	2.80	2.84	2.51	1.87	1.74	1.68	1.63	1.59	1.56	1.53	1.49	1.45	1.47	1.58	1.70	1.84	2.04	2.37
345	2.46	2.47	2.48	2.52	2.58	2.68	2.78	2.85	2.62	2.00	1.85	1.77	1.71	1.67	1.63	1.58	1.53	1.49	1.50	1.61	1.75	1.94	2.31	2.44
350	2.45	2.44	2.45	2.48	2.54	2.64	2.76	2.85	2.72	2.13	1.96	1.87	1.80	1.75	1.69	1.64	1.59	1.53	1.54	1.66	1.84	2.13	2.43	2.46
355	2.42	2.40	2.40	2.43	2.50	2.60	2.73	2.85	2.80	2.27	2.07	1.97	1.90	1.83	1.77	1.70	1.64	1.58	1.59	1.73	1.98	2.40	2.47	2.45
360	2.38	2.35	2.35	2.38	2.45	2.56	2.69	2.83	2.87	2.41	2.19	2.08	1.99	1.92	1.85	1.77	1.70	1.64	1.65	1.84	2.20	2.49	2.47	2.42

Figure-14: Launch window analysis on accumulated time in eclipse (% over the transfer time) for a typical GTO to GEO transfer, for different launch epochs & times

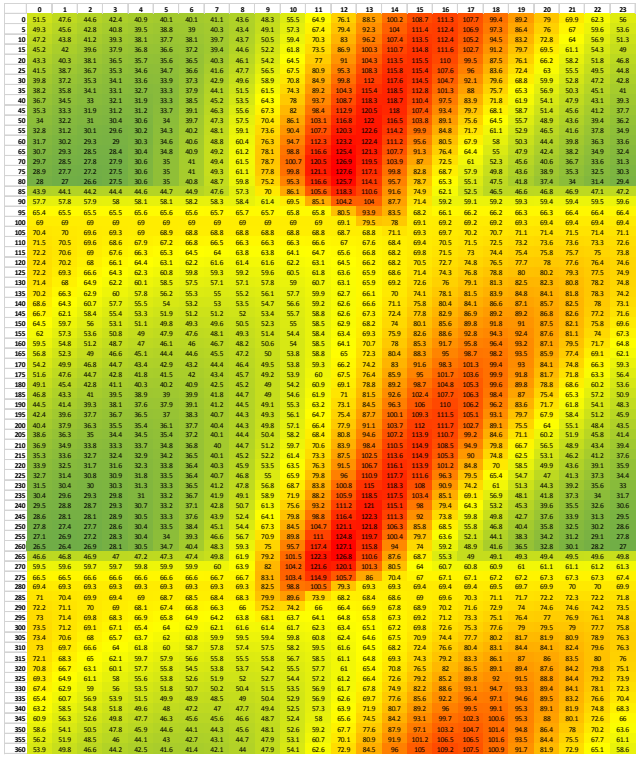

Figure-15: Launch window analysis for the longest eclipse for a typical GTO to GEO transfer, for different launch epochs & times

6. CONCLUSIONS

An indirect method (Sequential Gradient Restoration Algorithm) has been used for the generation of nominal low-thrust transfer trajectories and Δv budget analysis. The constraint that electric propulsion is off during eclipses was included in the tool: this was done by analytically solving for the quartic giving the intersection between two ellipses, to compute the starting and ending points for the eclipse. The approach was tested on multiple transfer scenarios, providing satisfactory performance in terms of accuracy, stability and computational time.

The output of the optimiser is then processed to obtain all the relevant performance indicators of a transfer such as eclipse duration, spacecraft angular velocity, AOCS variables, SADM rotation, sensor blinding, GEO ring crossings, etc. The tool offers also the possibility of running launch window analyses and obtain general results related to epoch-dependent phenomena such as eclipses and sensor blinding.

Finally, and for the generation of AOCS flyable profiles, a dedicated smoothing algorithm allows for the generation of angular momentum & torque compatible dynamics, while at the same time respecting the optimal solution provided by the tool.

7. REFERENCES

[1] P. B. de Selding, *SES Jumps on Electric-propulsion Bandwagon with Latest Satellite Order*, 17 July 2014, http://spacenews.com/41288ses-jumps-on-electric-propulsion-bandwagon-with-latest-satellite/ (accessed 01.09.2017)

[2] S. Clark, *Boeing first two all-electric satellites ready for launch*, 1 March 2015, https://spaceflightnow.com/2015/03/01/boeings-first-two-all-electric-satellites-ready-for-launch/ (accessed 01.09. 2017)

[3] A. Miele, R.E. Pritchard, J.N. Damoulakis, *Sequential Gradient Restoration Algorithm for Optimal Control Problems*, Journal of Optimization Theory and Applications 5, n. 4 (1970) 235–282

[4] R.A. Broucke, P.J. Cefola, *On the equinoctial orbit elements*, Celestial Mechanics 5 (1952) 303-310

[5] D. A. Danielson, C. P. Sagovac, B. Neta, L. W. Early, *Semi-analytic satellite theory*, Naval Postgraduate School, 2010

[6] *Quartic function*, https://en.wikipedia.org/wiki/Quartic_function

[7] P. Penarroya, J.C. Bastante, F. De Bruijn, C. Palm, *On the smoothing of slewing profiles for low thrust transfer trajectories*, 69th IAC Bremen, October 2018.

[8] F. Letizia, F. De Bruijn, J.C. Bastante, B. Lübke-Ossenbeck, *Optimisation tool for low thrust orbit raising based on the Sequential Gradient Restoration Algorithm*, 68th IAC Adelaide, September 2017